LANDAU LEVELS AND HALL EFFECT IN TWO DIMENTIONAL SYSTEMS

BY

BELAYNEH SEWNET MENGESTIA

A THESIS SUBMITED IN PARTIAL FULFILMENT OF THE REQUIREMENTS FOR THE DEGREE OF MASTER OF SCIENCE IN PHYSICS

AT

ADDIS ABABA UNIVERSITY

ADDIS ABABA, ETHIOPIA

JUNE 2014

ADDIS ABABA UNIVERSITY

COLLEGE OF NATURAL SCIENCE

DEPARTMENT OF PHYSICS

The undersigned hereby certify that they have read and recommended to the graduate committee of the department for acceptance a thesis entitled "LANDAU LEVELS AND HALL EFFECT IN TWO DIMENTIONAL SYSTEMS" by Belayneh Sewnet in partial fulfillment of the requirements for the degree of Master of Science in physics.

Signed by the Examination Committee:

Advisor: ______________________ Signature: _____________ Date: _____________

Examiner: ____________________ Signature: _____________Date: _____________

Examiner: ____________________ Signature: _____________Date: _____________

THIS THESIS DEDICATED TO MY FAMILY

Abstract

In this thesis, we represent Classical Hall Effect and Quantum Hall Effect studies at high magnetic field and low temperature in 2DEG and in high quality and charge carrier bilayer graphene samples for the degenerate Landau levels, with a particular emphasis on Integer and Fractional Quantum Hall effects. And also we have studied about the equation of quantization energy (Landau levels) by using Landau gauge and symmetric gauge solutions in 2DEG and bilayer graphene samples.

In 2DEG and in bilayer graphene, the thermal energy is less than quantization energy (k_BT $\ll \hbar\, \omega_c$) and degeneracy (g) is greater than or equal to total number of electrons. In this situation Quantum Hall Effect can be observed with quantized Hall resistances and plateaus for integer and fractional filing factor.

Acknowledgements

I would like to express my sincere thanks to my advisor and instructor Prof. Vadim N.Mal'nev for his guidance, assistance, supervision and contribution of valuable suggestions. His scientific excitement, integral view on research and overly enthusiasm, has made a deep impression on me. I would like to thank to all my friends for providing encouragement and support.

Table of contents

Chapter 4

Chapter 5

Chapter 6

List of Figures

Introduction

The Hall Effect was discovered in 1879 by Edwin Hall. While running a current through a sample of semiconductor with an applied magnetic field, he measured two voltages, one parallel to the current path and one across the current path. He found that when the magnetic field was applied perpendicular to the sample the voltage measured across the sample V_{xy}, also denoted V_H for Hall voltage [1].

Hall's observation can be understood as the Lorentz force bending the electron paths from the longitudinal direction to the transverse direction. When a perpendicular magnetic field and an in-plane current is applied to a sample of semiconductor, it causes an accumulation of negative charge (electrons) on one side of the sample and an equivalent positive charge (holes) on the opposite side, in the case of negatively charged carriers. This introduces an electric field in the transverse direction E_y. When the pile up of electrons on the one side of the sample is big enough for E_y to cancel out the Lorentz force due to the magnetic field, the electrons will again on average move in the longitudinal direction [1, 2].

A century after Edwin Hall found R_H to be linearly proportional to the strength of the magnetic field, Klaus von Klitzing and collaborators in 1980 found that in two dimensions at very low temperatures and high magnetic fields observed a stepwise dependence of R_H on magnetic field strength with plateaus [1]. These plateaus were accompanied by a simultaneous drop of the magneto resistance R_{xx} to zero, at sufficiently low temperatures. What Von Klitzing and collaborators observed was the Quantum Hall effect, an effect which is observable in two dimensional electron systems including two dimensional electron gas (like Si-MOSFET and a GaAs/AlGaAs samples) and latter in the graphene samples.

The fundamental properties of the QHE are a consequence of the fact that the energy spectrum of the electronic system used for the experiments is a discrete energy spectrum. If the energy for the motion in one direction (usually z-direction) is fixed, and apply a strong magnetic field perpendicular to the two-dimensional plane will lead to a quantized energy spectrum or electron distributes in Landau levels and then at low temperature(k_BT $<<$ $\hbar\omega_c$) all electrons fill at lowest state, which is necessary for the observation of the Quantum Hall effect.

The plot of resistivity versus applied magnetic field strength becomes an increasing series of plateaus. This implied that in quantum mechanics, resistance is quantized in units of $\frac{h}{\upsilon e^2}$(where h is Planck constant, υ is filling factor and e is electron charge), the plateaus corresponded to the cases where the resistivity was related to the magnetic field by integer and fractional values of filling factor. These integer and fractional values led to the theory of the Integer Quantum Hall Effect and the Fractional Quantum Hall Effect. Both of these effects have since been observed in 2DEG and in graphene [3, 4].

Chapter 1

Classical Hall Effect

As we introduced above, Edwin Hall observed that when an electrical current passes through a semiconductor sample placed in a magnetic field, a potential proportional to the current and to the magnetic field is developed across the material in a direction perpendicular to both the current and to the magnetic field [5]. A particle with charge e moving with a velocity $\vec{v}(t)$ in a uniform magnetic field $\vec{\mathrm{B}}$ will experience a Lorentz force $\vec{\mathrm{F}}$,

$$\vec{\mathrm{F}} = \mathrm{m}\,\dot{\vec{v}}(t) = e\vec{\mathrm{E}}(t) + \frac{e}{c}\vec{v}(t) \times \vec{\mathrm{B}} \quad (1.1)$$

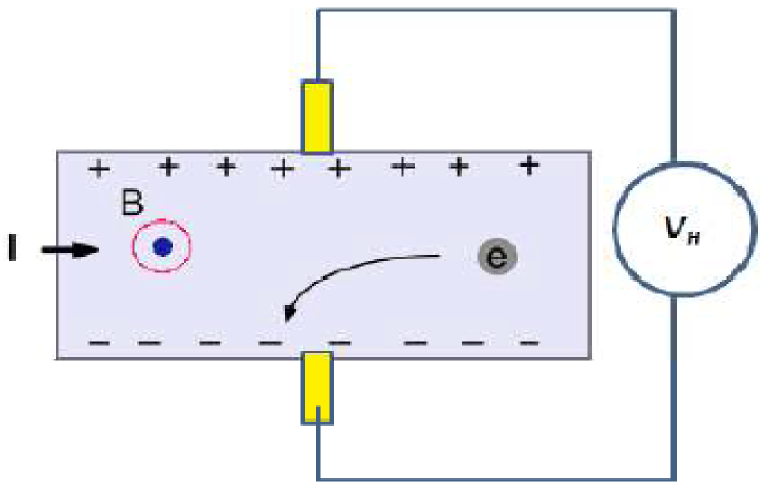

Figure: 1.1 Classical Hall Effect.

When an external magnetic field is applied perpendicularly to a current carrying conductor, the charges experience the Lorentz force and are defected to one side of the conductor. Then, equal but opposite charges accumulate on the opposite side. The result is an asymmetric distribution of charge carriers on the conductor's surface. This separation of charges establishes an electric field that opposes further separation of charge. As long as charges flow, a steady electric potential exists called the Hall voltage and the resistivity of the conductor depends linearly on the magnetic field strength. This is known as the Classical Hall Effect.

So the solutions of equations (1.1) can be obtained as follows,

Let the electric field in *x*, *y* and *z* direction be

$$\left.\begin{aligned} \mathrm{E}_x(t) &= \mathrm{E}_{ox}e^{-i\omega t} \\ \mathrm{E}_y(t) &= \mathrm{E}_{oy}e^{-i\omega t} \\ \mathrm{E}_z(t) &= \mathrm{E}_{oz}e^{-i\omega t} \end{aligned}\right\}. \quad (1.2)$$

and velocity in *x*, *y* and *z* direction be

$$\left.\begin{aligned} v_x(t) &= v_{ox}e^{-i\omega t} \\ v_y(t) &= v_{oy}e^{-i\omega t} \\ v_z(t) &= v_{oz}e^{-i\omega t} \end{aligned}\right\}. \quad (1.3)$$

From the cross product $(\vec{v}(t)\times\vec{\mathrm{B}})$ one obtains *x*, *y* and *z* components as $(v(t)\times\mathrm{B})_x = \mathrm{B}v_y(\mathrm{t})$, $(v(t)\times\mathrm{B})_y = -\mathrm{B}v_x(\mathrm{t})$ and $(v(t)\times\mathrm{B})_z = 0$

Then by using equation (1.2) and equation (1.1) with matrix results, electron moving equations can be written as

$$\left.\begin{aligned} m\dot{v}_x(t) &= e\,E_{ox}e^{-\iota\omega t} + \frac{e\mathrm{B}}{c}v_y(t) \\ m\dot{v}_y(t) &= e\,E_{oy}e^{-\iota\omega t} - \frac{e\mathrm{B}}{c}v_x(t) \\ m\dot{v}_z(t) &= e\,E_{oz}e^{-\iota\omega t} \end{aligned}\right\}. \quad (1.4)$$

First by using *x* and *y* components of equation (1.3) and equation (1.4), we get system equations for unknown v_{ox} and v_{oy} like

$$v_{ox} = \frac{ie}{\omega m}E_{ox} + \frac{i\omega_c}{\omega}v_{oy}. \quad (1.5)$$

$$\nu_{oy} = \frac{ie}{\omega m} E_{oy} - \frac{i\omega_c}{\omega} \nu_{ox} \tag{1.6}$$

where $\omega_c = \frac{e\text{B}}{mc}$ is cyclotron frequency.

Now we substitute equation (1.6) in to equation (1.5) to get ν_{ox}

$$\nu_{ox} = \frac{i\omega e}{m(\omega^2 - \omega_c^2)} E_{ox} - \frac{\omega_c e}{m(\omega^2 - \omega_c^2)} E_{oy}. \tag{1.7}$$

And we substitute equation (1.5) in to equation (1.6) to get ν_{oy}

$$\nu_{oy} = \frac{\omega_c e}{m(\omega^2 - \omega_c^2)} E_{ox} + \frac{i\omega e}{m(\omega^2 - \omega_c^2)} E_{oy}. \tag{1.8}$$

Also from *z* components of equation (1.3) and equation (1.4) we can get ν_{oz}

$$\nu_{oz} = \frac{ie}{\omega m} E_{oz}. \tag{1.9}$$

To calculate conductivity tensor, first we have to evaluate current density in *x*, *y* and *z* direction from current equation

$$\vec{\text{J}}(\text{t}) = \text{e}\, n_c \vec{v}(\text{t}). \tag{1.10}$$

where n_c is density number of particle (carrier density).

So that current density of *x*, *y* and *z* components can be written

$$\text{J}_x(\text{t}) = \frac{i n_c \omega e^2}{m(\omega^2 - \omega_c^2)} E_x(\text{t}) - \frac{n_c \omega_c e^2}{m(\omega^2 - \omega_c^2)} E_y(\text{t}). \tag{1.11}$$

$$\text{J}_y(\text{t}) = \frac{n_c \omega_c e^2}{m(\omega^2 - \omega_c^2)} E_x(\text{t}) + \frac{i n_c \omega e^2}{m(\omega^2 - \omega_c^2)} E_y(\text{t}). \tag{1.12}$$

$$\text{J}_z(\text{t}) = \frac{i n_c e^2}{\omega m} E_z(\text{t}). \tag{1.13}$$

Using ohm's low we can write tensor equation as

$$\text{J}_i = \sigma_{ij} \text{E}_j.$$

Finally, by using tensor equation and comparing equation (1.11), (1.12) and (1.13) we can get conductivity tensor,

$$\begin{pmatrix} \sigma_{xx} & \sigma_{xy} & \sigma_{xz} \\ \sigma_{yx} & \sigma_{yy} & \sigma_{yz} \\ \sigma_{zx} & \sigma_{zy} & \sigma_{zz} \end{pmatrix} = \begin{pmatrix} \frac{in_c\omega e^2}{m(\omega^2-\omega_c^2)} & -\frac{n_c\omega_c e^2}{m(\omega^2-\omega_c^2)} & 0 \\ \frac{n_c\omega_c e^2}{m(\omega^2-\omega_c^2)} & \frac{in_c\omega e^2}{m(\omega^2-\omega_c^2)} & 0 \\ 0 & 0 & \frac{in_c e^2}{\omega m} \end{pmatrix}. \quad (1.14)$$

From this equation the hall resistance $\rho_{xy} = \sigma_{xy}{}^{-1}$ is

$$\sigma_{xy}{}^{-1} = -\frac{m(\omega^2-\omega_c^2)}{n_c\omega_c e^2},$$

$$\sigma_{xy}{}^{-1} = \frac{-m\omega^2 + m\omega_c^2}{n_c\omega_c e^2},$$

Let $\omega \to 0$(electric filed is constant and does not depend on ω)

$$\sigma_{xy}{}^{-1} = \frac{m\omega_c}{n_c e^2}$$

$$= \frac{m}{n_c e^2}\frac{\mathrm{B}e}{mc} = \frac{\mathrm{B}}{n_c ec}. \quad (1.15)$$

And the Hall coefficient ($\mathrm{R_H}$) can be written as,

$$\mathrm{R_H} = \frac{1}{\sigma_{xy}\mathrm{B}} = \frac{1}{n_c ec}. \quad (1.16)$$

According to equation (1.16) the lower the carrier density the greater the magnitude of $\mathrm{R_H}$ will be obtained. This follows from the fact that the lower the density the fewer electrons have to generate the same current and hence the faster the electrons will have to move. Electrons with bigger velocities (magnitude) experience stronger Lorentz forces and hence give rise to a bigger Hall voltage. Due to its simple form, and easy practical realization, the Hall resistance has become a standard tool for determining the carrier density of electrical carriers. In addition the Hall Effect distinguishes between negatively and positively charged carriers.

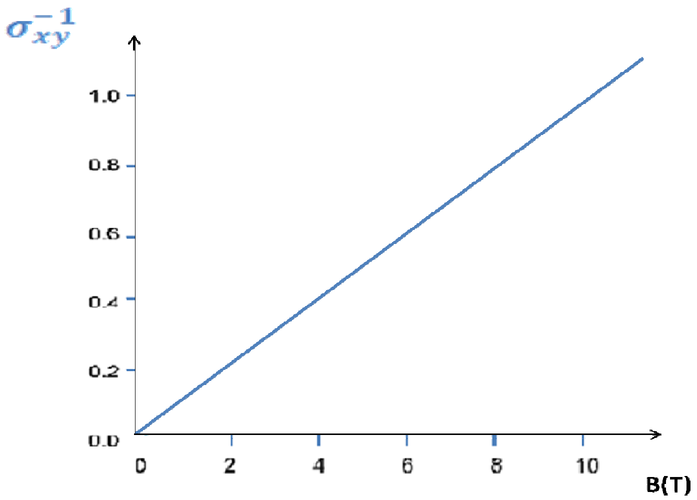

Figure: 1.2 Graph of classical Hall Effect, it shows Hall resistance $\sigma_{xy}{}^{-1}$ has linear relation with magnetic field B.

Also we consider cross-sectional area of the sample A = ab and the current $\mathrm{I}_x(\mathrm{t})$ is the product of current density $\mathrm{J}_x(\mathrm{t})$ and cross-sectional area A,

$$\mathrm{I}_x(\mathrm{t}) = \mathrm{J}_x(\mathrm{t})\,\mathrm{A}$$
$$= n_c \mathrm{e}\, v_x(\mathrm{t})\,\mathrm{A},$$

From this equation we can write $v_x(\mathrm{t})$ as

$$v_x(\mathrm{t}) = \frac{\mathrm{I}_x(\mathrm{t})}{n_c \mathrm{eA}}.$$

And electric field in the y direction is

$$\mathrm{E}_y(t) = v_x(t)\mathrm{B},$$
$$= \frac{\mathrm{I}_x(\mathrm{t})\,\mathrm{B}}{n_c \mathrm{eA}}. \qquad (1.17)$$

In an experiment, one can measure the potential difference across the sample-the Hall voltage $\mathrm{V_H}$ and also we can calculate from electric field across the sample, which is related to the Hall field by equation;

$$\mathrm{V_H} = -\int_0^{\mathrm{a}} \mathrm{E}_y(t)\,dy,$$

$$= - \frac{I_x(t)Ba}{n_c eab},$$

$$= - (\frac{1}{n_c e})\frac{I_x(t)B}{b}. \quad (1.18)$$

In Classical Hall Effect, the Hall voltage depends on both the external magnetic field and the driving current, linear dependence of Hall voltage on the current intensity through the sample. Classical Hall Effect determines the carrier charges concentration in the material (sample), in addition determine the dependence of drop voltage (or current intensity – these two measures are linearly correlated) on temperature, at constant driving current and the dependence Hall voltage (current intensity) on temperature.

From a practical perspective, the Hall Effect allows the construction of sensitive devices for measuring the magnetic field induction, namely Hall probes.

Chapter 2

Two Dimensional Electron Gas (2DEG)

As a harbinger of things to come, in 1966 Shubnikov– de Haas oscillations were observed in 2DEG in a silicon metal-oxide-semiconductor field-effect transistor (MOSFET) [6]. The electrons free to move in two dimensions and the energy without magnetic field is quasicontinuous and can be compared with the kinetic energy of free electrons with wave vector $\vec{k}$ but with an effective mass *m*.*

From the general Schrödinger equation;

$$\mathrm{E(k)}\psi(r) = \frac{-\hbar^2}{2m^*}\vec{\nabla}^2\,\psi(r)$$

And the solution of equation,

$$\psi(\vec{r}) = \mathrm{A}_n e^{i(k_x x + k_y y + k_z z)},$$

$$\mathrm{E(k)}e^{i(k_x x + k_y y + k_z z)} = \left(\frac{\partial^2}{\partial x^2} + \frac{\partial^2}{\partial y^2} + \frac{\partial^2}{\partial z^2}\right)e^{i(k_x x + k_y y + k_z z)}$$

We get the parabolic energy dispersion of 2DEG as

$$\mathrm{E(k)} = \frac{\hbar^2 k^2}{2m^*}.$$

where - $k^2 = k_x^2 + k_y^2 + k_z^2$,

- $m^* \approx 0.1m_e$ is the effective mass of the free electron for 2DEG (effective mass is known from band structure calculation),
- m_e is the mass of the free electron.

2.1. Landau Levels in 2DEG

In this section we consider the behavior of electron gas in constant magnetic field with the help of quantum mechanics. In strong magnetic fields electrons undergo cyclotron orbits, due to the Lorentz force. The quantization of these cyclotron orbits is called Landau quantization. It restricts the charged particles to orbits with discrete energy values - the so called Landau levels [7]. In the case originally considered by Landau, the external potential is assumed to vanish (V = 0, no electric field and apply magnetic field along *z*-direction).

The Hamiltonian of 2DEG doesn't depend on *x* component, we get a plane wave solution in the *x*-direction, and in the *y*-direction the problem in the Landau gauge ($\mathbf{A} = A_x$, 0, 0) becomes equivalent to one dimensional harmonic oscillator potential [8].

Free electron with effective mass m^* and charge *e*, moving in the xy-plane under the influence of a magnetic field B_z is described by the Hamiltonian [9].

$$\widehat{H} = \frac{1}{2m^*}(\hat{p} - \frac{e}{c}\vec{A})^2. \tag{2.1.1}$$

Landau quantization energy of 2DEG can be obtained from Schrödinger equation with Hamiltonian equation (2.1.1),

$$\frac{1}{2m^*}(\hat{p} - \frac{e}{c}\vec{A})^2\,\psi(x, y) = E\psi(x, y). \tag{2.1.2}$$

We can get equation of Landau levels from equation (2.1.2) by using Landau gauge in rectangular coordinate, where there is one component of vector potential, taking $\vec{A} = (A_x, 0, 0)$. In this case the vector potential can be expressed as $A_x = -yB_o$, $A_y = A_z = 0$ and magnetic field from $\vec{B} = \vec{\nabla} \times \vec{A}$ with Landau gauge vector potentials we have only $B_z = B_o$.

Schrödinger equations with Landau gauge vector potential we can written as

$$\frac{1}{2m^*}[(\hat{p}_x + \frac{e}{c}yB_o)^2 + \hat{p}_y^2]\psi(x,y) = E\psi(x,y). \qquad (2.1.3)$$

The solution of equation (2.1.3) is

$$\psi(x,y) = A_n e^{ikx}\,\varphi(y).$$

Equation (2.1.3) with solution can be written as,

$$\frac{1}{2m^*}[(\hat{p}_x + \frac{e}{c}yB_o)^2 + \hat{p}_y^2]A_n e^{ikx}\varphi(y)) = E\,A_n\,e^{ikx}\varphi(y). \qquad (2.1.4)$$

Now by substituting $\hat{p}_x = \hbar k$ and $\hat{p}_y = \frac{\hbar}{i}\frac{d}{dy}$, one obtains

$$\frac{1}{2m^*}[\left(\hbar k + \frac{e}{c}yB_o\right)^2 - \hbar^2\frac{d^2}{dy^2}]\,e^{ikx}\varphi(y)) = E\,e^{ikx}\varphi(y),$$

$$[\frac{d^2}{dy^2} + \frac{2m^*}{\hbar^2}(E - \frac{m^*\omega_c^2}{2}(y - (\frac{-\hbar kc}{eB_o}))^2)]\varphi(y) = 0,$$

$$[\frac{d^2}{dy^2} + \frac{2m^*}{\hbar^2}(E - \frac{m^*\omega_c^2}{2}(y - y_o)^2)]\varphi(y) = 0. \qquad (2.1.5)$$

where, $\omega_c = \frac{eB_o}{m^*c}$, cyclotron frequency

$y_o = \frac{-\hbar kc}{eB_o}$, center position,

Let us introduce dimensionless coordinate as $y = \alpha\xi$, where α has dimenssion of length and ξ is dimensionless coordinate.

So equation (2.1.5) can be presented as

$$[\frac{d^2}{d\xi^2} + \frac{2m^*}{\hbar^2}\alpha^2 E - \frac{2m^*\omega_c^2\alpha^4}{2\hbar^2}(\xi - \xi_o)^2]\varphi(\xi) = 0. \qquad (2.1.6)$$

By setting $\frac{2m^*\omega_c^2\alpha^4}{2\hbar^2} = 1$, we get $\alpha = \sqrt{\frac{\hbar}{m^*\omega_c}}$, and rewrite equation (2.1.6) as

$$[\frac{d^2}{d\xi^2} + \frac{2m^*}{\hbar^2}\alpha^2\text{E} - (\xi - \xi_o)^2]\varphi(\xi) = 0,$$

$$[\frac{d^2}{d\xi^2} + \frac{2m^*\text{E}}{\hbar^2}\frac{\hbar}{m^*\omega_c} - (\xi - \xi_o)^2]\varphi(\xi) = 0,$$

$$[\frac{d^2}{d\xi^2} + \frac{2\text{E}}{\hbar\omega_c} - (\xi - \xi_o)^2]\varphi(\xi) = 0,$$

$$[\frac{d^2}{d\xi^2} + \lambda - (\xi - \xi_o)^2]\varphi(\xi) = 0, \tag{2.1.7}$$

where $\lambda = \frac{2\text{E}}{\hbar\omega_c}$.

From finite solution of free electrons harmonic oscillation we have $\lambda = 2n + 1$ and by comparing with $\lambda = \frac{2\text{E}}{\hbar\omega_c}$, we can get

$$\frac{2\text{E}}{\hbar\omega_c} = 2n + 1,$$

$$\text{E}_n = \hbar\omega_c\left(n + \frac{1}{2}\right), \tag{2.1.8}$$

with $n = 0, 1, 2\ldots$

Therefore quantization energy dispersion of 2DEG is the equation of harmonic oscillator. The kinetic energy of a charged particle in the xy-plane is quantized in the external magnetic field and the separation between the nearest quantum levels is $\hbar\omega_c$. Equation (2.1.8) is known as the Landau formula which describes equidistant quantum spectrum of a charged particle in an external magnetic field. This energy spectrum is called Landau levels.

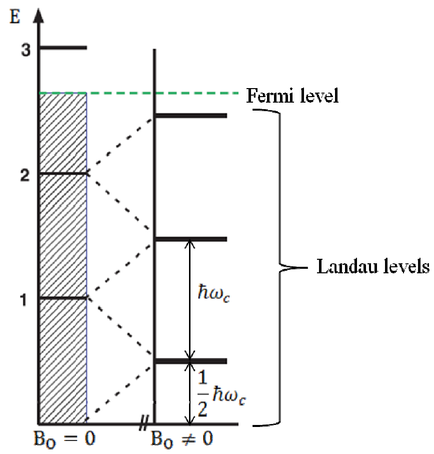

Figure: 2.1.1 Landau levels in two dimensional electron gases with magnetic field.

And eigenfunction of 2DEG can be written with Rodriguez formula and Hermit polynomial as,

$$\varphi_n(y) = N_n \exp\left(-\frac{m^*\omega_c}{2\hbar}(y-y_o)^2\right) H_n\left[\sqrt{\frac{m^*\omega_c}{\hbar}}(y-y_o)\right].$$

Here we introduce $N_n = \frac{1}{\sqrt{2^n n! \pi^{1/2}}}$ normalization constant.

So that eigenfunction of corresponding energy dispersion becomes

$$\psi_{nk}(x,y) = \frac{1}{\sqrt{2^n n! \pi^{1/2}}} \exp(ikx) \exp\left(-\frac{m^*\omega_c}{2\hbar}(y-y_o)^2\right) H_n\left[\sqrt{\frac{m^*\omega_c}{\hbar}}(y-y_o)\right]. \tag{2.1.9}$$

Here H_n is Hermite polynomial.

From equation (2.1.8 and 2.1.9) we see that the energy depends on n only but wave function depends on n and k_y, which means for the energy level n we get degenerate states with different k_y or the number of possible states in a Landau level, i.e. the degree of degeneracy is given by the possible values of k_y. When periodic boundaries are assumed, the quantization of the k_y quantum number is given by,

$$k_y = \frac{2\pi}{L_y} n_y, \quad \text{where } n_y = 0, 1, 2 \ldots.$$

Number of possible wave functions n_y is

$$n_y = \frac{L_y}{2\pi}\, k_y,$$

We have $y_0 = -\frac{\hbar k c}{e B_o}$, and when we put $y_0 = L_x$ we get maximum value of k_y like,

$$k_y = \frac{e B_0 L_x}{\hbar c},$$

And also for maximum k_y we have degeneracy of Landau levels $g = n_y$,

$$g = n_y = \frac{L_y}{2\pi}\, k_y = \frac{L_x L_y e B_0}{2\pi\hbar c} = \frac{A B_0}{hc/e} = \frac{\phi}{\phi_o},$$

$$g = \frac{\phi}{\phi_o}. \qquad (2.1.11)$$

where A - Surface area of sample,

h - Planck's constant,

ϕ - Total applied flux (magnetic flux through the surface),

ϕ_o - Quantum of magnetic flux (elementary flux). The magnetic flux is quantized in units of $\frac{hC}{e}$.

This equation (2.1.11) shows that the degeneracy is directly proportional to the magnetic field strength. At high magnetic field, the separation and degeneracy of the Landau levels are higher. It is important to note that the position of the Fermi energy must be determined from the charge carrier density. The density of states at Fermi levels changes as a function of magnetic field, as the magnetic field is raised from zero; the separation between the Landau levels grows and so does the number of states that each level holds or the levels became distinct when (k_BT $\ll \hbar\omega_c$) [9], this means the effects of Landau quantization are only observed when the thermal energy is smaller than the separation energy of the Landau levels. If k_BT $\ll \hbar\omega_c$, all electrons lie on the lowest Landau level provided that the degeneracy (g) is greater than or equals to the total number of electrons. In this case we can observe Quantum Hall Effect.

$$\mathrm{T} << \frac{\hbar\omega_c}{k_B} = \frac{\hbar e \mathrm{B_o}}{k_B m^*}, \text{ where } \omega_c = \frac{e\mathrm{B_o}}{m^*}$$

Numerical value of magnetic length a_H for higher magnetic field $\mathrm{B_o} = 10\mathrm{T}$ is

$$a_H = \sqrt{\frac{\hbar}{eB_o}} = \sqrt{\frac{1.05\times10^{-34} Js}{1.6\times10^{-19} C\times 10\mathrm{T}}} = 8\mathrm{nm}$$

And temperature T $<< \frac{\hbar e \mathrm{B_o}}{k_B m^*}$, for $\mathrm{B_o} = 1\mathrm{T}$ is

$$\mathrm{T} << \frac{\hbar e \mathrm{B_o}}{k_B m^*}, = \frac{1.85\times10^{-22}\mathrm{J}}{1.38\times10^{-23} JK^{-1}} \approx 10\mathrm{K}$$

This means, QHE can be observed in 2DEG when the temperature of the sample is much less than 10K.

Chapter 3

Quantum Hall Effect in 2DEG

The Quantum Hall Effect is a quantum mechanical version of the Hall effect, observed in 2DEG subjected to low temperature and strong magnetic field, in which the Hall resistivity takes on the quantized values $R_{xy} = \frac{h}{\upsilon e^2}$.

The Quantum Hall effect is referred to as the Integer or Fractional Quantum Hall Effect depending on whether ($\upsilon = \frac{hn_c}{e\mathrm{B_o}}$) is an integer or fraction respectively. QHE explained in terms of electron orbital's in a magnetic field, i.e. from Landau levels at high magnetic field and low temperature we can observe plateaus with quantized value of Hall resistivity.

3.1. Integer Quantum Hall Effect in 2DEG

Klaus von Klitzing, Michael Pepper, and Gerhardt Dordda firstly observed IQHE, truly remarkable at low temperatures (~4K) and high magnetic fields (10T) [10], the Hall resistance of a two dimensional electron system is found to have plateaus at the exact values of $R_{xy} = \frac{h}{\upsilon e^2}$, filing factor is an integer.

At the same time, in the applied magnetic field range where the Hall resistance shows the plateaus, the longitudinal resistance vanishes.

i.e. $R_{xx} = \frac{V_x}{I_x} \rightarrow 0$, and $R_{xy} = \frac{h}{\upsilon e^2} = \frac{h}{e^2}\frac{eB_o}{hn_c} = \frac{B_o}{en_c}$.

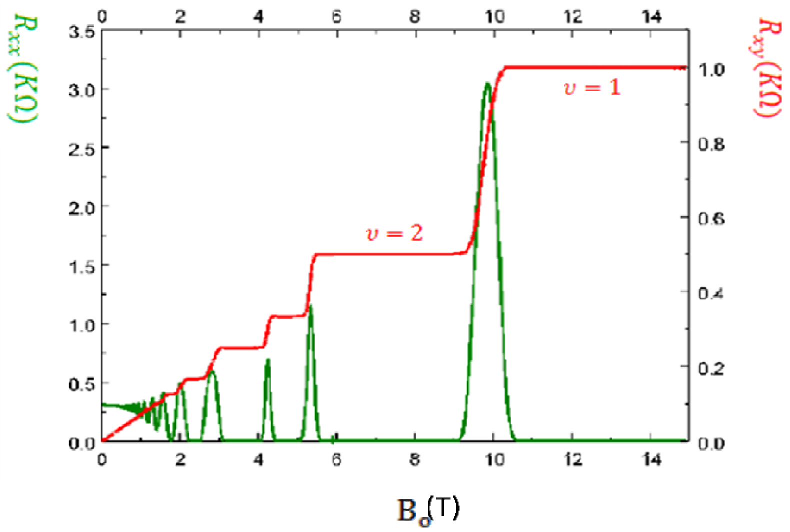

Figure: 3.1.1 Graph of Integer Quantum Hall Effect in 2DEG

Which is determined purely by the fundamental Planck's constant h and charge of electron e, for $\upsilon = 1$ one obtains the value $R_{xy} = \frac{h}{e^2} =$ 25.8128 … kΩ [10, 11].

This means, it can be measured so precisely that the QHE has become the resistance standard and the Hall Effect is the standard way of measuring the concentration of carriers in semiconductor.

The fine structure constant is one of the key fundamental constants and it plays a very important role in quantum electrodynamics. In CGS unit, the fine structure constant is $\boldsymbol{\alpha} = \frac{\mu_0 ce^2}{2h} = \frac{1}{137}$ and it can be deduced from the QHE [11].

If $\boldsymbol{\alpha} = 0$, the electrons that do not interact with each other (a free electron system). If $\boldsymbol{\alpha}$ is very large, the electrons have very strong interactions with each other. In reality, $\boldsymbol{\alpha} \sim \frac{1}{137}$, which is small but nonzero. It means the electron interacts, but the coupling is very weak.

3.2. Fractional Quantum Hall Effect in 2DEG

Two years later, the even more intriguing FQHE was discovered by Horst L. Störmer, Daniel C. Tsui, and Arthur C. Gossard. When 2DEG was cooled down below (~2K) [12, 13], FQHE seen only at low temperature in sample and strong magnetic field (10T) with very high mobility, and all electrons are in the lowest landau levels when $\upsilon \leq 1$.

The Hall resistance of the 2DEG shows plateaus at the values of $\frac{h}{\upsilon e^2}$, instead of stopping at υ =1, plateaus continue to fractional values of $\upsilon = \frac{p}{q}$ where q is an odd integer, Such as $\frac{1}{3}$, $\frac{1}{7}$, $\frac{2}{3}$, $\frac{4}{5}$ and so on.

The first observed fractional state, $\upsilon = \frac{1}{3}$, was explained by Laughlin's approximate many-body ground state, which describes the correlated motion of the interacting electron system [14].

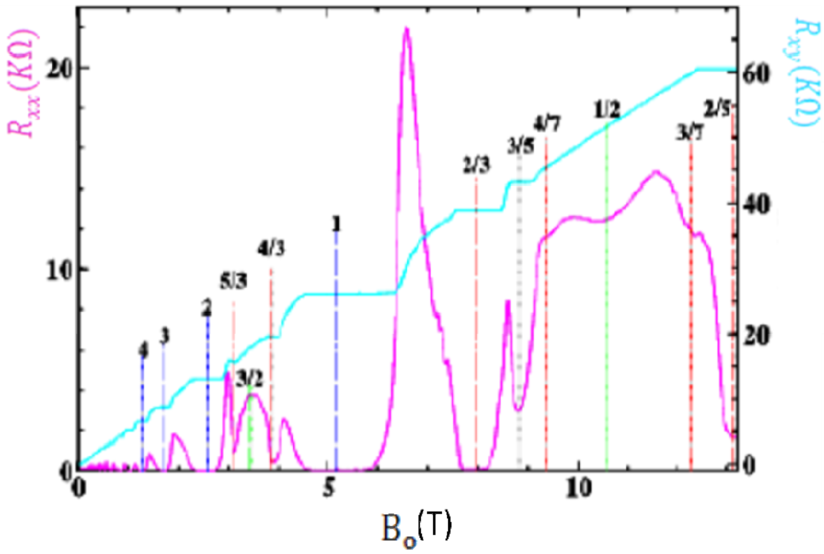

Figure: 3.2.1 Graph of Fractional Quantum Hall Effect in 2DEG.

In the above graph, we have two types of filling factors, the first one is between 1 and 2 ($\frac{4}{3}$, $\frac{3}{2}$ and $\frac{5}{3}$), the second one is less than one ($\frac{2}{3}$, $\frac{3}{5}$, $\frac{4}{7}$, $\frac{1}{2}$, $\frac{3}{7}$, and $\frac{2}{5}$). All these fractional filing factors can form plateaus with Hall resistivity.

Chapter 4

Graphene

4.1. Monolayer graphene

The energy spectrum of electrons in 2D hexagonal lattice had already been studied theoretically in 1947 by P.R. Wallace [15], He predicted that the electron spectrum of 2D hexagonal lattice has the linear dependence of the wave vector *k*. The wave equation for excitations was written down by J.W. McClure [16]. Already in 1956, and the similarity to the Dirac equation was discussed by G.W. Semenoff and also DiVincenzo and E.J.Mele in 1984 [17, 18].

Andre Geim, Konstantin Novoselov and their collaborators, presented their results on graphene structures in October of 2004 [19]. i.e. they isolated graphene is a monolayer of graphite and graphene is packed into a hexagonal lattice, with a carbon-carbon distance of 0.142 nm that can be viewed as either an individual atomic plane extracted from graphite or unrolled single-wall carbon nanotubes or as a giant flat fullerene molecule.

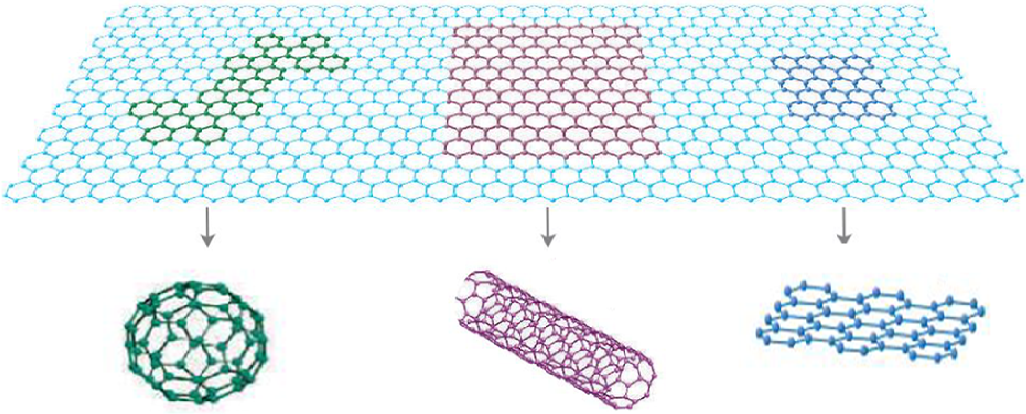

Figure: 4.1.1 Monolayer graphene structures

Undoped monolayer graphene has a Fermi energy coinciding with the energy at the conical points, with a completely filled valence band, an empty conduction band and no band gap in between. This means that, monolayer graphene is an example of a gapless semiconductor, in which low-energy quasiparticles within each valley can formally be described by the Dirac-like Hamiltonian[20].

$$\hat{\mathrm{H}} = v_F \begin{pmatrix} 0 & (\hat{p}_x - i\hat{p}_y) \\ (\hat{p}_x + i\hat{p}_y) & 0 \end{pmatrix} \qquad (4.1.1)$$

Here $v_F = 10^6 m/s$ is the Fermi velocity.

The eigenfunction of monolayer graphene is given by

$$\psi_{e,h}(\vec{k}) = \frac{e^{i\vec{k}.\vec{r}}}{\sqrt{2}} \begin{pmatrix} e^{-i\phi_{\vec{k}}/2} \\ \pm e^{i\phi_{\vec{k}}/2} \end{pmatrix}. \qquad (4.1.2)$$

where $\phi_{\vec{k}}$ is the polar angle of vector $\vec{k}$ and *e*,*h* represents electron and hole.

For monolayer graphene, the massless Dirac fermions are described by a linear dispersion relations $E_{e,h} = \pm \hbar v_F k$.

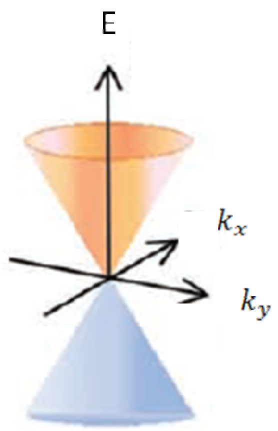

Figure: 4.1.2 Linear energy dispersions of monolayer graphene for zero magnetic fields.

The density of states D(E) vanishes at E = 0, and which gives the number of available electronic states per energy and space, in single layer graphene is unusual for a 2D system with an energy dependence [21].

Density of state at conical point, $D_k = \frac{kdk}{\pi}$

$$D(E) = \frac{EdE}{\pi \hbar^2 v_f^2}$$

Where $k = \frac{E}{\hbar^2 v_f^2}$

Since there are two Dirac pointes

$$D(E) = \frac{2}{\pi \hbar^2 v_f^2} |E|.$$

4.2. Bilayer graphene

Consider now the case of bilayer graphene (Novoselov et al., 2006; McCann and Falko, 2006; McCann, Abergel and Falko, 2006).

Bilayer graphene consists of two honeycombs of carbon atoms with lattice structure of AA stacking and AB stacking (Bernal stacking), for Bernal stacking the bottom layer A_2 atom sits right under the top layer B_1.

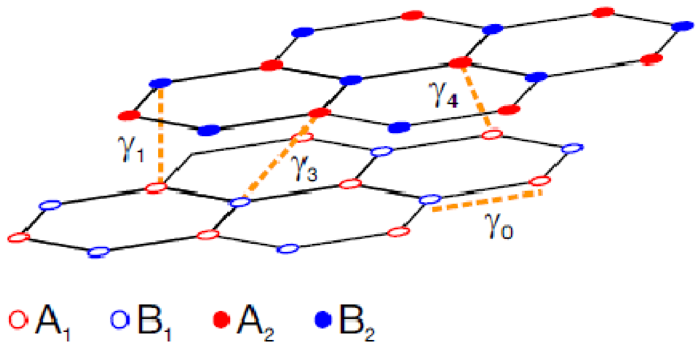

Figure: 4.2.1 Bilayer graphene lattice in Bernal stacking, with the hopping parameters γ_0 (A − B), γ_1 ($A_1 - B_2$), γ_3 ($B_1 - A_2$) and γ_4 ($A_1 - A_2$, $B_1 - B_2$).

In the bilayer graphene with AB stacking, most important inter-layer interaction is given by the nearest-neighbor hopping γ_1. Within this approximation, the effective Hamiltonian is written as [20],

$$\widehat{\mathrm{H}} = \frac{1}{2m^*}\begin{pmatrix} 0 & (\hat{p}_x - i\hat{p}_y)^2 \\ (\hat{p}_x + i\hat{p}_y)^2 & 0 \end{pmatrix}. \qquad (4.2.1)$$

This is a new type of quantum mechanical Hamiltonian that is different both from non-relativistic (Schrödinger) and from relativistic (Dirac) cases. Also eigenfunctions of bilayer graphene is given by

$$\psi_{e,h}(\vec{k}) = \frac{e^{i\vec{k}.\vec{r}}}{\sqrt{2}} \begin{pmatrix} e^{-i\phi_{\vec{k}}} \\ \pm e^{i\phi_{\vec{k}}} \end{pmatrix}. \quad (4.2.2)$$

When the potential difference between the layers is zero, the dispersion relation becomes parabolic with energy dispersion $E_{e,h} = \pm \frac{\hbar^2 k^2}{2m^*}$.

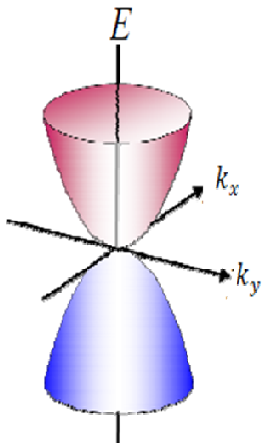

Figure: 4.2.2 Parabolic energy dispersions of bilayer graphene for zero magnetic fields.

The density of states, is constant in bilayer graphene [21]

$$D(E) = \frac{2m^*}{\pi\hbar^2} = \text{constant}$$

4.3. Landau Levels in bilayer graphene

We have a two dimensional Hamiltonian to describe the energy electronic excitations of a bilayer graphene, which correspond to quasiparticles with a parabolic energy dispersion. Its high magnetic field Landau level spectrum consists of almost equidistant groups of fourfold degenerate state at finite energy and eight degenerate states at zero energy [22]. This can be translated into the Hall conductivity dependence on carrier density, which exhibits plateaus at $\sigma_{xy} = \frac{\upsilon e^2}{h}$ with integer and fractional values of filing factor υ.

4.3.1. Solution in Landau gauge (Rectangular coordinate)

To obtain the Landau level in bilayer graphene by using Landau gauge solutions in rectangular coordinate system, we choose potential $\mathrm{A} = (\mathrm{A}_x, 0, 0)$ to represent magnetic field [9], this means the vector potentials, $\mathrm{A}_x = -\mathrm{yB_o}$, $\mathrm{A}_y = \mathrm{A}_z = 0$ and $\mathrm{B} = \mathrm{B}_z$.

The Hamiltonian of bilayer graphene with Landau gauge vector potential is,

$$\widehat{\mathrm{H}} = \frac{1}{2m^*}\begin{pmatrix} 0 & (\hat{p}_x - i\hat{p}_y + \frac{e}{c}y\mathrm{B_o})^2 \\ (\hat{p}_x + i\hat{p}_y + \frac{e}{c}y\mathrm{B_o})^2 & 0 \end{pmatrix}. \quad (4.3.1.1)$$

Schrödinger equation with Hamiltonian can be written as

$$\frac{1}{2m^*}\begin{pmatrix} 0 & (\hat{p}_x - i\hat{p}_y + \frac{e}{c}y\mathrm{B_o})^2 \\ (\hat{p}_x + i\hat{p}_y + \frac{e}{c}y\mathrm{B_o})^2 & 0 \end{pmatrix}\begin{pmatrix}\psi_1(x,y) \\ \psi_2(x,y)\end{pmatrix} = \mathrm{E}\begin{pmatrix}\psi_1(x,y) \\ \psi_2(x,y)\end{pmatrix}, \quad (4.3.1.2)$$

And also it can be written as a form of

$$\left.\begin{matrix} \frac{1}{2m^*}(\hat{p}_x - i\hat{p}_y + \frac{e}{c}y\mathrm{B_o})^2\psi_2(x,y) = \mathrm{E}\psi_1(x,y) \\ \frac{1}{2m^*}(\hat{p}_x + i\hat{p}_y + \frac{e}{c}y\mathrm{B_o})^2\psi_1(x,y) = \mathrm{E}\psi_2(x,y) \end{matrix}\right\}. \quad (4.3.1.3)$$

From equation (4.3.1.3), one obtains $\psi_1(x,y)$ and $\psi_2(x,y)$ as

$$\left.\begin{aligned} \psi_2(x,y) &= \frac{1}{2m^*\mathrm{E}}\left[(\hat{p}_x + i\hat{p}_y + \frac{e}{c}y\mathrm{B_o})^2\right]\psi_1(x,y) \\ \psi_1(x,y) &= \frac{1}{2m^*\mathrm{E}}\left[(\hat{p}_x - i\hat{p}_y + \frac{e}{c}y\mathrm{B_o})^2\right]\psi_2(x,y) \end{aligned}\right\}. \tag{4.3.1.4}$$

And by substituting $\psi_2(x,y)$ from equation (4.3.1.4) in to equation (4.3.1.3) first part we can get,

$$\frac{1}{2m^*}(\hat{p}_x - i\hat{p}_y + \frac{e}{c}y\mathrm{B_o})^2\frac{1}{2m^*E}(\hat{p}_x + i\hat{p}_y + \frac{e}{c}y\mathrm{B_o})^2\psi_1(x,y) = \mathrm{E}\psi_1(x,y). \tag{4.3.1.5}$$

By substituting $\hat{p}_x = \hbar k$ and $\hat{p}_y = \frac{\hbar}{i}\frac{d}{dy}$ in equation (4.3.1.5), we can obtains

$$(\hbar k - \frac{i\hbar}{i}\frac{d}{dy} + \frac{e}{c}y\mathrm{B_o})^2(\hbar k + \frac{i\hbar}{i}\frac{d}{dy} + \frac{e}{c}y\mathrm{B_o})^2\varphi_1(y) = 4E^2m^{*2}\varphi_1(y),$$

$$(k - \frac{d}{dy} + \frac{e}{\hbar c}y\mathrm{B_o})^2(k + \frac{d}{dy} + \frac{e}{\hbar c}y\mathrm{B_o})^2\varphi_1(y) = \frac{4\mathrm{E}^2m^{*2}}{\hbar^4}\varphi_1(y),$$

$$(-\frac{d}{dy} + \frac{eB_o}{\hbar c}(\frac{k\hbar c}{e\mathrm{B_o}} + y))^2(\frac{d}{dy} + \frac{eB_o}{\hbar c}(\frac{k\hbar c}{e\mathrm{B_o}} + y))^2\varphi_1(y) = \frac{4E^2m^{*2}}{\hbar^4}\varphi_1(y),$$

$$(-\frac{d}{dy} + \frac{1}{a_H^2}(y - y_o))^2(\frac{d}{dy} + \frac{1}{a_H^2}(y - y_o))^2\varphi_1(y) = \frac{4\mathrm{E}^2m^{*2}}{\hbar^4}\varphi_1(y),$$

where, $a_H^2 = \frac{\hbar c}{e\mathrm{B_o}}$, a_H is magnetic length.

Now we can introduce dimensionless coordinate $\mathrm{y} = \alpha\xi$, (where α has dimenssion of length and ξ is dimensionless coordinate), and we can obtains,

$$(-\frac{1}{\alpha}\frac{d}{d\xi} + \frac{\alpha}{a_H^2}(\xi - \xi_o))^2(\frac{1}{\alpha}\ \frac{d}{d\xi} + \frac{\alpha}{a_H^2}(\xi - \xi_o))^2\varphi_1(\xi) = \frac{4\mathrm{E}^2 m^{*2}}{\hbar^4}\varphi_1(\xi),$$

Here we can use, $\xi_o = -k\sqrt{\frac{\hbar c}{e\mathrm{B_o}}} = -ka_{H.}$

Then multiplying both side by α and by equating $\alpha = a_H$, we can get

$$(-\frac{d}{d\xi} + (\xi))^2(\frac{d}{d\xi} + (\xi))^2\varphi_1(\xi) = \frac{4\mathrm{E}^2 m^{*2}\alpha^4}{\hbar^4}\varphi_1(\xi). \qquad (4.3.1.6)$$

From this equation we can introduce new dimensionless operators like

$$\hat{a}^+ = \frac{1}{\sqrt{2}}(-\frac{d}{d\xi} + \xi),$$

$$\hat{a} = \frac{1}{\sqrt{2}}(\frac{d}{d\xi} + \xi),$$

So equation (4.3.1.6) with new dimensionless operator can be written as,

$$(\hat{a}^+)^2(\hat{a})^2 = \frac{\mathrm{E}^2 m^{*2}\alpha^4}{\hbar^4},$$

$$(\hat{a}^+)^2(\hat{a})^2 = \frac{\mathrm{E}^2 m^{*2}}{\hbar^4}\frac{\hbar^2}{m^{*2}{\omega_c}^2},$$

where $\alpha^4 = \frac{\hbar^2}{m^{*2}{\omega_c}^2}$,

$$(\hat{a}^+)^2(\hat{a})^2 = \frac{\mathrm{E}^2}{\hbar^2{\omega_c}^2}. \qquad (4.3.1.7)$$

From commutation relation of dimensionless operators we have

$$[n, \hat{a}^+] = \hat{a}^+$$

Here $n = \hat{a}^+\hat{a}$

$$n\hat{a}^{+} - \hat{a}^{+}n = \hat{a}^{+},$$

$$\hat{a}^{+}\hat{a}\ \hat{a}^{+} = \hat{a}^{+}\hat{a}^{+}\hat{a} + \hat{a}^{+},$$

Using $\hat{a}^{+}\hat{a} = \hat{a}\hat{a}^{+} - 1$ and $\hat{a}\hat{a}^{+} = \hat{a}^{+}\hat{a} + 1$ relations we obtains

$$(\hat{a}^{+})^{2}(\hat{a})^{2} = n^{2} - n. \tag{4.3.1.8}$$

Finally from equation (4.3.1.7) and equation (4.3.1.8) we can get

$$\frac{\mathrm{E}^{2}}{\hbar^{2}\omega_{c}^{2}} = n^{2} - n,$$

So quantization energy of bilayer graphene is

$$\left.\begin{array}{ll} \mathrm{E}_{n} = \pm\hbar\omega_{c}\sqrt{n(n-1)}, & \text{for } n \geq 2, \\ \mathrm{E}_{n} = 0, & \text{for } n = 0 \text{ and } 1, \end{array}\right\}. \tag{4.3.1.9}$$

This means, in bilayer graphene there is two different energy levels, the first one is zero energy level for n is 0 and 1and the second one is infinite energy levels for $n \geq 2$.

Landau levels - quantized energy spectrum of bilayer graphene with perpendicular applied magnetic field and the potential difference between the two layers is zero is shown in figure (4.3.1).

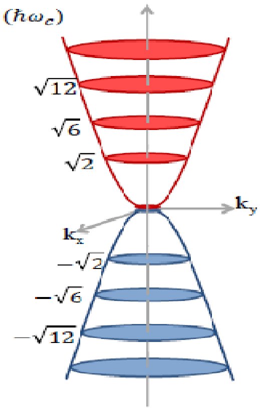

Figure: 4.3.1 Landau levels in bilayer graphene with magnetic field for differentn.

The Landau level spectrum of the Hamiltonian consists of a series of electron and hole levels with energies and wave functions [22] given by

$$\psi_{n,k}(x,y) = \mathrm{N}_n\, e^{\mathrm{ikx}} \begin{pmatrix} \varphi_{n,k} \\ \pm\varphi_{n-2,k} \end{pmatrix}, \quad \text{for } n \geq 2 \qquad (4.3.1.10)$$

$$\psi_{n,k}(x,y) = \mathrm{N}_n\, e^{\mathrm{ikx}} \begin{pmatrix} \varphi_{n,k} \\ 0 \end{pmatrix}, \quad \text{for } n = 0 \text{ and } 1 \qquad (4.3.1.11)$$

The energy is not depend on the quantum number k_y but eigenfunction depends on k_y this means Landau levels have large degeneracy because of different wave functions with different k_y values, in this case we can solve degeneracy using boundary conditions, so the solutions with boundary of L_y can be written as

$$\psi_{1,2}(x,y) = \psi_{1,2}(x, y + L_y),$$

And quantum number is, $k_y = \frac{2\pi}{L_y} n_y$,

$$n_y = \frac{k_y L_y}{2\pi},$$

where n_y is 0, 1, 2 ….

And maximum value of n_y is determined by the condition of the center of the orbit, $0 < x_0 < L_x$, so for maximum $k_y = \frac{eB_0 L_x}{\hbar c}$ and degeneracy $g = n_y$;

$g = \frac{\phi}{\phi_o}$ - degeneracy of bilayer graphene for $n \geq 2$, it is four fold degeneracy.

$g = \frac{2\phi}{\phi_o}$ - degeneracy of bilayer graphene for n is 0 and 1, this shows the degeneracy is double because Landau level degenerate for 0 or 1, it is eight fold degeneracy.

Landau quantization in bilayer graphene can be observed also at low temperature (~2K) and large magnetic field (10T); this means quantization only observed when the thermal energy is smaller than the separation energy of the Landau levels and degeneracy is greater than or equal to total number of electrons.

4.3.2. Solution in symmetric gauge (Cylindrical coordinate)

Hamiltonian of bilayer graphene in cylindrical coordinates of $\vec{R} = (r, \theta)$ is given by [23],

$$\widehat{\mathrm{H}} = \frac{-\hbar^2}{2m^*}\begin{pmatrix} 0 & (-ie^{-i\theta}(\frac{d}{dr} - \frac{i}{r}\frac{d}{d\theta}))^2 \\ (-ie^{i\theta}(\frac{d}{dr} + \frac{i}{r}\frac{d}{d\theta}))^2 & 0 \end{pmatrix}. \qquad 4.3.2.1)$$

For the solution of symmetric gauge in cylindrical coordinate (r, θ, z), we have potential $\vec{A} = \frac{1}{2}\vec{B} \times \vec{r}$ to represent magnetic field [6]. The line of $\vec{A}$ now form circles about the origin and cylindrical polar coordinate (r, θ) with $A_\theta = \frac{1}{2} B_o r$ and $A_r = A_z = 0$, so by using Schrödinger equation with symmetric gauge, we can solve the equation of quantization energy of bilayer graphene as follows,

$$\widehat{\mathrm{H}}\psi(r,\theta) = \mathrm{E}\,\psi(r,\theta).$$

$$\frac{-\hbar^2}{2m^*}\begin{pmatrix} 0 & (-ie^{-i\theta}(\frac{d}{dr} - \frac{i}{r}\frac{d}{d\theta} - \frac{eB_o r}{2\hbar c}))^2 \\ (-ie^{i\theta}(\frac{d}{dr} + \frac{i}{r}\frac{d}{d\theta} - \frac{eB_o r}{2\hbar c}))^2 & 0 \end{pmatrix}\begin{pmatrix} \psi_1(r,\theta) \\ \psi_2(r,\theta) \end{pmatrix}$$
$$= \mathrm{E}\begin{pmatrix} \psi_1(r,\theta) \\ \psi_2(r,\theta) \end{pmatrix}. \qquad (4.3.2.2)$$

And equation (4.3.2.2) can be written as a form of

$$\left.\begin{aligned} \frac{-\hbar^2}{2m^*}\left[(-ie^{-i\theta}(\frac{d}{dr} - \frac{i}{r}\frac{d}{d\theta} - \frac{eB_o r}{2\hbar c}))^2\right]\psi_2(r,\theta) = \mathrm{E}\psi_1(r,\theta) \\ \frac{-\hbar^2}{2m^*}\left[(-ie^{i\theta}(\frac{d}{dr} + \frac{i}{r}\frac{d}{d\theta} - \frac{eB_o r}{2\hbar c}))^2\right]\psi_1(r,\theta) = \mathrm{E}\psi_2(r,\theta) \end{aligned}\right\}. \qquad (4.3.2.3)$$

From equation (4.3.2.3) we have

$$\psi_2(r,\theta) = \frac{-\hbar^2}{\mathrm{E}2m^*}\left[(-ie^{i\theta}(\frac{d}{dr} + \frac{i}{r}\frac{d}{d\theta} - \frac{eB_o r}{2\hbar c}))^2\right]\psi_1(r,\theta). \qquad (4.3.2.4)$$

And by substituting equation (4.3.2.4) in to equation (4.3.2.3), we obtains

$$(-ie^{-i\theta}(\frac{d}{dr} - \frac{i}{r}\frac{d}{d\theta} - \frac{eB_0 r}{2\hbar c}))^2 \, (-ie^{i\theta}(\frac{d}{dr} + \frac{i}{r}\frac{d}{d\theta} + \frac{eB_0 r}{2\hbar c}))^2 \psi_1(r,\theta) = \frac{4E^2 m^{*2}}{\hbar^4}\psi_1(r,\theta). \quad (4.3.2.5)$$

Due to the cylindrical symmetry of the problem

$$\psi_1(r,\theta) = \varphi_1(r) e^{il\theta}$$

where l is integer angular quantum number.

Substitute $\psi_1(r,\theta)$ in equation (4.3.2.5), we can get

$$\left[-\frac{d^2}{dr^2} - \frac{2l}{r}\frac{d}{dr} + \frac{l}{r^2} - \frac{l^2}{r^2} + \frac{lm^*\omega_c}{\hbar} + \frac{m^*\omega_c}{2\hbar} - \frac{m^{*2}\omega_c^2 r^2}{4\hbar^2} + \frac{m^*\omega_c r}{2\hbar}\frac{d}{dr}\right]\left[\frac{d^2}{dr^2} - \frac{2l}{r}\frac{d}{dr} + \frac{l}{r^2} + \frac{l^2}{r^2} + \frac{lm^*\omega_c}{\hbar} + \frac{m^*\omega_c}{2\hbar} + \frac{m^{*2}\omega_c^2 r^2}{4\hbar^2} + \frac{m^*\omega_c r}{2\hbar}\frac{d}{dr}\right]\varphi_1(r) = \frac{4E^2 m^{*2}}{\hbar^4}\varphi_1(r). \quad (4.3.2.6)$$

Let us introduce dimensionless coordinate for radial part, $r = \alpha\xi$ and substitute it in equation (4.3.2.6)

$$\left[-\frac{1}{\alpha^2}\frac{d^2}{d\xi^2} - \frac{2l}{\alpha^2\xi}\frac{d}{d\xi} + \frac{l}{\alpha^2\xi} - \frac{l^2}{\alpha^2\xi^2} + \frac{lm^*\omega_c}{\hbar} + \frac{m^*\omega_c}{2\hbar} - \frac{m^{*2}\omega_c^2\xi^2}{4\hbar^2} + \frac{m^*\omega_c\alpha\xi}{2\hbar\alpha}\frac{d}{d\xi}\right]\left[\frac{1}{\alpha^2}\frac{d^2}{d\xi^2} - \frac{2l}{\alpha^2\xi}\frac{d}{d\xi} + \frac{l}{\alpha^2\xi} + \frac{l^2}{\alpha^2\xi^2} + \frac{lm^*\omega_c}{\hbar} - \frac{m^*\omega_c}{2\hbar} + \frac{m^{*2}\omega_c^2\xi^2}{4\hbar^2} + \frac{m^*\omega_c\alpha\xi}{2\hbar\alpha}\frac{d}{d\xi}\right]\varphi_1(\xi) = \frac{4E^2 m^{*2}}{\hbar^4}\varphi_1(\xi) \quad (4.3.2.7)$$

Multiplying by α^2 both side and by equating $\alpha = a_H$, we get

$$\left[-\frac{d^2}{d\xi^2}-\frac{2l}{\xi}\frac{d}{d\xi}+\frac{l}{\xi^2}-\frac{l^2}{\xi^2}+l-\frac{\xi^2}{4}+\frac{\xi}{2}\frac{d}{d\xi}+\frac{1}{2}\right]\left[\frac{d^2}{d\xi^2}-\frac{2l}{\xi}\frac{d}{d\xi}-\frac{l}{\xi^2}+\frac{l^2}{\xi^2}+l+\frac{\xi^2}{4}-\frac{\xi}{2}\frac{d}{d\xi}-\frac{1}{2}\right]\varphi_1(\xi)=\frac{4\mathrm{E}^2m^{*2}\alpha^4}{\hbar^4}\varphi_1(\xi),$$

$$\left[\left(-\frac{d^2}{d\xi^2}-\frac{\xi^2}{4}+\frac{1}{2}\right)-\frac{2l}{\xi}\frac{d}{d\xi}-\frac{l^2}{\xi^2}-\frac{l}{\xi^2}+l\right]\left[-\left(-\frac{d^2}{d\xi^2}-\frac{\xi^2}{4}+\frac{1}{2}\right)-\frac{2l}{\xi}\frac{d}{d\xi}+\frac{l^2}{\xi^2}-\frac{l}{\xi^2}+l\right]\varphi_1(\xi)=\frac{4\mathrm{E}^2}{\hbar^2{\omega_c}^2}\varphi_1(\xi). \qquad (4.3.2.8)$$

Equation (4.3.2.8) with angular solution can be written as follows

$$\mathrm{E}^2=\hbar^2{\omega_c}^2\left[\frac{1}{2}\left(-\frac{d}{d\xi}+\xi\right)\left(\frac{d}{d\xi}+\xi\right)-1+\frac{|l|}{2}-\frac{l}{2}\right]\left[\frac{1}{2}\left(-\frac{d}{d\xi}+\xi\right)\left(\frac{d}{d\xi}+\xi\right)+\frac{|l|}{2}-\frac{l}{2}\right]. \qquad (4.3.2.9)$$

Now we can introduce new dimensionless operators for radial coordinate as

$$\hat{b}^+=\frac{1}{\sqrt{2}}(-\frac{d}{d\xi}+\xi),$$

$$\hat{b}=\frac{1}{\sqrt{2}}(\frac{d}{d\xi}+\xi),$$

And we can write equation (4.3.2.9) as follows

$$\mathrm{E}^2=\hbar^2{\omega_c}^2\left[\hat{b}^+\hat{b}-1+\frac{|l|}{2}-\frac{l}{2}\right]\left[\hat{b}^+\hat{b}+\frac{|l|}{2}-\frac{l}{2}\right]. \qquad (4.3.2.10)$$

Then equation (4.3.2.10) with radial quantum number $n_r=\hat{b}^+\hat{b}$, can be written as

$$\mathrm{E}^2=\hbar^2{\omega_c}^2(n_r-1+\frac{|l|}{2}-\frac{l}{2})(n_r+\frac{|l|}{2}-\frac{l}{2})$$

Finally using new quantum number $n = n_r + \frac{|l|}{2} - \frac{l}{2}$, we obtains the energy spectrum or 2D harmonic oscillator equation

$$\left.\begin{array}{ll} \mathrm{E}_n = \pm\hbar\omega_c\sqrt{n(n-1)}, & \text{for } n \geq 2, \\ \mathrm{E}_n = 0, & \text{for } n = 0 \text{ and } 1, \end{array}\right\}. \qquad (4.3.2.11)$$

In this case we have $n = n_r$ for $l > 0$ and $n = n_r + |l|$ for $l < 0$, so in the case of $l < 0$ we have degeneracy for different n and l values.

Now we can write the wave functions with symmetric gauge eigenenergies by using associated Laguerre polynomial and Rodriguez formula (without normalization) for holes and electrons like

$$\psi_{n,l}(r,\theta) = e^{il\theta}\exp(-\frac{r^2}{4}\frac{m\omega_c}{\hbar})r^{|l|}L_n^{(|l|)}(\frac{r^2}{2}\frac{m\omega_c}{\hbar}) \qquad (4.3.2.11)$$

where $L_n^{(|l|)}$ is associated Laguerre polynomial.

4.4. A unified description of monlayer and bilayer grapphene

Consider now the case of magnetic fields large enough that, $|\mathrm{E}| \geq |t_\perp|$, (where $t_\perp = \Gamma\sqrt{\frac{2|e|\hbar B v_f^2}{c}}$ it describes the coupling between layers), at these energies a parabolic dispersion transforms to a conical one [20].

The 4×4 Hamiltonian is

$$\hat{\mathrm{H}} = \begin{pmatrix} 0 & v_f\hat{\pi}_+ & t_\perp & 0 \\ v_f\hat{\pi}_- & 0 & 0 & 0 \\ t_\perp & 0 & 0 & v_f\hat{\pi}_- \\ 0 & 0 & v_f\hat{\pi}_+ & 0 \end{pmatrix}. \tag{4.4.1}$$

Using dimensionless units $\hat{\pi}_\pm = \hat{\pi}_x \pm i\hat{\pi}_y = \hat{b}_\pm\sqrt{\frac{2|e|\hbar \mathrm{B}}{c}}$ and $\mathrm{E} = \varepsilon\sqrt{\frac{2|e|\hbar \mathrm{B} v_f^2}{c}}$, one can represent the Schrödinger equation with the Hamiltonian,

$$\left.\begin{array}{c} \hat{b}\psi_2(\mathrm{x,y}) + \Gamma\psi_3(\mathrm{x,y}) = \varepsilon\psi_1(\mathrm{x,y}) \\ \hat{b}^+\psi_1(\mathrm{x,y}) = \varepsilon\psi_2(\mathrm{x,y}) \\ \Gamma\psi_1(\mathrm{x,y}) + \hat{b}^+\psi_4(\mathrm{x,y}) = \varepsilon\psi_3(\mathrm{x,y}) \\ \hat{b}\psi_3(\mathrm{x,y}) = \varepsilon\psi_4(\mathrm{x,y}) \end{array}\right\}. \tag{4.4.2}$$

On excluding $\psi_2(\mathrm{x,y})$ and $\psi_4(\mathrm{x,y})$, one obtains

$$\left.\begin{array}{c} \frac{1}{\varepsilon}\hat{b}\hat{b}^+\psi_1(\mathrm{x,y}) + \Gamma\psi_3(\mathrm{x,y}) = \varepsilon\psi_1(\mathrm{x,y}) \\ \Gamma\psi_1(\mathrm{x,y}) + \frac{1}{\varepsilon}\hat{b}^+\hat{b}\psi_3(\mathrm{x,y}) = \varepsilon\psi_3(\mathrm{x,y}) \end{array}\right\}. \tag{4.4.3}$$

On replacing $\hat{b}^+\hat{b}$ by n and $\hat{b}\hat{b}^+$by n+1, we find the eigenenergies for both of monolayer and bilayer graphene.

$$\varepsilon_n^2 = \frac{\Gamma^2 + 2n+1}{2} \pm \sqrt{(\frac{\Gamma^2 + 2n+1}{2})^2 - n(n+1)}. \tag{4.4.4}$$

For $\Gamma = 0$, we can get Landau level as

$$\varepsilon_n^2 = n + \frac{1}{2} \pm \frac{1}{2}. \tag{4.4.5}$$

And for large Γ also we have

$$\varepsilon_{n1}^2 = \frac{n(n+1)}{\Gamma^2}. \tag{4.4.6}$$

Equation (4.4.6) gives the Landau levels for low-lying bands in the parabolic approximation.

$$\varepsilon_{n2}^2 = \Gamma^2 + 2n + 1. \tag{4.4.7}$$

And equation (4.4.7) is the Landau levels for two-gapped bands in the parabolic approximation.

Chapter 5

Quantum Hall Effect in bilayer graphene

5.1. Anomalous Quantum Hall Effects in bilayer graphene

The QHE in bilayer graphene assumes that all the states between Landau levels are localized due to disorder; this means that, if the Fermi energy lies between the Landau levels, then only the states belonging to the occupied Landau levels contribute to the transport.

The Landau quantization of charge carrier Dirac fermions with finite mass results in plateaus in Hall conductivity at standard integer positions but the last (zero-level) plateau is missing. The zero-level anomaly is accompanied by metallic conductivity in the limit of low concentrations and high magnetic fields, in stark contrast to the conventional, insulating behavior in this regime. The zero energy levels ($n = 0$ and 1) are responsible for unconventional quantization of Integer Quantum Hall Effect, with Hall conductivity of $\sigma_{xy} = \mathrm{g}_s \mathrm{g}_\mathrm{v} n \frac{e^2}{h} = 4n \frac{e^2}{h}$,

Where g_s and g_v are spin degeneracy and valley degeneracy respectively, and $\mathrm{g}_s = \mathrm{g}_\mathrm{v} \approx 2$, wit account of this we have Hall conductivity;

$$\sigma_{xy} = 4n \frac{e^2}{h} = \upsilon \frac{e^2}{h},$$

Here $\upsilon = 4n = \pm 4, \pm 8, \pm 12 \ldots$

5.2. Fractional Quantum Hall Effect in bilayer graphene

Theoretical scientists expect that electrons in graphene are strongly interacting and hence exhibit FQHE. The FQHE depends upon the combined effect of the magnetic field and coulomb interaction between electrons. The FQHE occurs when the magnetic field is so strong, that the plateaus occurred at fractional values of the filling factor, because fractional values of the filling factor refers to partially filled Landau states. In this case, for non interacting electrons the ground state is macroscopically degenerate. It is the Coulomb interaction between the electrons that lifts the degeneracy and opens a gap [24]. Therefore the origin of the FQHE cannot be understood based on the behavior of individual electrons in a magnetic field; it is the behavior of all the electrons [25].

For interacting bilayer graphene, an important characteristic is that it is a semiconductor with a tunable band gap between the valence and conduction bands [26]. This property modifies the Landau level spectrum and influences the role of long-range Coulomb interactions [27].

The excitation gaps of the FQHE states depend on the magnetic field, the bias voltage, and the Landau level index. Therefore, the electron-electron interaction properties of a bilayer graphene can be controlled by the external parameters. By varying these parameters the excitation gap of the FQHE states can therefore be controlled, this means excitation gap and the FQHE states of bilayer graphene have dependence on the value of magnetic field, applied base voltage and Landau level index n [28, 29].

At the zero bias voltage, the Landau levels become two-fold valley and two-fold spin degenerate and are given by the expression, Since the FQHE is expected only in the Landau levels with low values of the index, we consider below the sets of Landau levels of bilayer graphene with $n = 0$ and 1 only. The stable FQHE states in a bilayer graphene are expected for the $n = 0$ and $n = 1$ Landau level sets. In these Landau levels the FQHE gap does not depend on the bias voltage. For all other levels the FQHE gap depends on the bias voltage, which clearly illustrates the sensitivity of the interaction properties on the external parameters. The interaction strength within a single Landau level can be controlled by the bias voltage.

Chapter 6

Possible application of graphene and QHE

The physical properties of bilayer graphene are excellent electrical conductivity with room temperature mobility up to $40{,}000 cm^2 \mathrm{V}^{-1} s^{-1}$ in air and high thermal conductivity with room temperature termal conductivity of about 2,800 $m^{-1}\mathrm{K}^{-1}$ [30, 31, 32], the possibility to tune electrical properties by changing the carrier density through gating or doping [33], mechanical stiffness, strength and flexibility(Young's modulus is estimated to be about 0.8TPa) [34, 35], transparency with transmittance of white light of about 95% [36] and impermeability to gases [37].

Since graphene is a transparent conductor it can be used in applications such as touch screens, light panels and solar cells, where it can replace the rather fragile and expensive Indium-Tin-Oxide, flexible electrodes for touch screen displays [38], high-frequency transistors [39], thermoelectric devices [40], photonic and plasmonic devices [41] and photo detectors [42], energy applications including batteries [43, 44], and new types of composite materials based on graphene with great strength and low weight could also become interesting for use in satellites and aircraft [45, 46].

There are many applications of QHE, for example, a measurement of the fine structure constant and successful application in metrology for the development of a primary alternate current (ac) resistance standard. It will simplify the link between resistance and capacitance and improve the measurement capabilities in the field of impedance measurements [47].

Conclusion

Classical Hall Effect, when an external magnetic field is applied perpendicularly to a current carrying conductor, the charges experienced the Lorentz force and equal but opposite charges accumulate on the opposite side of conductor. The result is an asymmetric distribution of charge carriers on the conductor's surface. This separation of charges establishes an electric field that opposes further separation of charge and the resistivity of the conductor has linear depends on the magnetic field strength.

The 2DEG in a magnetic field, in order to satisfy the minimum energy principle, the electrons will fill the Landau levels starting from the lowest energy level. In most of the cases, a number of Landau levels will be completely filled, and the highest Landau level will be partially occupied. The Fermi energy is the energy of the last Landau level in which electrons reside.

The energy of a 2DEG is not continuous under a perpendicular magnetic field, but the number of total quantum states should be the same as that without magnetic field, which means the Landau level is degenerate.

At very low temperatures and high magnetic fields (up to 10T), the thermal excitations between Landau levels are negligible. If the magnetic field is increased, the capacity of each Landau level will increase, and electrons from higher levels will drop to lower Landau levels until they are filled again. If one continues to increase the magnetic field, the highest Landau level will be depleted, while all the levels below are exactly filled. The Fermi energy of the system will drop suddenly and QHE observes.

The basic QHE experimental observation is the nearly vanishing longitudinal resistance $R_{xx} \to 0$ and the quantization of the Hall resistance $R_{xy} = \frac{h}{\upsilon e^2}$ of a two dimensional electron gas subjected to a strong magnetic field, the filing factor υ could take on integer value for IQHE and fractional values FQHE. Fractional Quantum Hall Effect is the result of involving strong Coulomb interactions and correlations among the electrons.

Bilayer graphene QHE behavior reveals the existence of Dirac fermions with finite mass, which are distinct from other known quasiparticles. The unconventional QHE in bilayer graphene originates from peculiar properties of its charge carriers that are Dirac fermions with finite mass.

The existence of a double degenerate Landau level explains the unconventional QHE found in bilayer graphene. This Landau level lies at the border between electron and hole gases and, taking into account the quadruple degeneracy, the existence of such Landau level implies that there must be a QHE step across the neutrality point.

Due to the double degeneracy, it takes twice the amount of carriers to fill it (as compared to all other Landau levels), so that the transition between the corresponding QHE plateaus must be twice wider. Also, the step between the plateaus must be twice higher, that is $\frac{8e^2}{h}$ as compared to $\frac{4e^2}{h}$ for the other steps at higher carrier densities.

In bilayer graphene, the FQHE depends upon the combined effect of the magnetic field and electron-electrons. The FQHE occurs when the magnetic field is so strong, that the plateaus occurred at fractional values of the filling factor, because fractional values of the filling factor refers to partially filled Landau states, and non interacting electrons the ground state is macroscopically degenerate.

It is the Coulomb interaction between the electrons that lifts the degeneracy and opens a gap. For Landau levels in bilayer graphene the excitation gaps of the FQHE states depend on the magnetic field, the bias voltage, and the Landau level index, therefore by varying these parameters the excitation gap of the FQHE states can be controlled.

Bibliography

[1]. [Horst L. Störmer. Nobel lecture: The fractional quantum hall effect. Reviews of Modern Physics, **71**(4), July 1999]

[2]. [Charles Kitte, Introduction to Solid State Physics, John Wiley & Sons, Inc, 2005.]

[3]. [K. von Klitzing, et al. Phys. Rev. Lett. **45**, 494 (1980)]

[4]. [J. K. Jain, Composite Fermions. Cambridge University Press, Cambridge, NY, 2007]

[5]. [Hall, E. H., on a new action of the magnet on electric currents", American Journal of Mathematics **2**, No. 3, (1879)]

[6]. [A. B. Fowler, F. F. Fang, W. E. Howard, and P. J. Stiles, Phys. Rev. Lett. **16** (1966), No. 20, 901].

[7]. [L. D. Landau, Z. Phys., **64**, (1930), 629]

[8]. [Vol.3 Quantum mechanics, Non-relativistic theory, 3rd Ed.]

[9]. [Physics of Low-dimensional Semiconductors - An Introduction John H. Davies, Cambridge University Press (2006)]

[10]. [K. Klitzing, G. Dorda and M. Pepper Phys. Rev. Lett. **45**, 494 (1980)]

[11]. [Volume **45**, number 6, Physical. Review Letters 11 august (1980)]

[12]. [D. C. Tsui, H. L. Störmer and A. C. Gossard Phys. Rev. Lett. **48**, 1559(1982)]

[13]. [J. P. Eisenstein and H. L. Störmer Science, 1510, (22 June 1990)]

[14]. [R. B. Laughlin. Anomalous quantum Hall Effect, an incompressible quantum fluid with fractionally charged excitations. Physical Review Letters **50**, 1395, (1983)]

[15]. [P. R. Wallace, Physical Review **71**, 476 (1947)]

[16]. [J. W. McClure, Physical Review **104**, 666 (1956)]

[17]. [G. W. Semenoff, Physical Review Letters **53**, 2449 (1984)]

[18]. [D. P. DiVincenzo and E. J. Mele, Phys. Rev. B **29**, 1685 (1984)]

[19]. [K. S. Novoselov *et al.*, Science **306**, 666 (2004)].

[20]. [Mikhail I. Katsnelson-Graphene_ Carbon in Two Dimensions, Cambridge University Press (2012)]

[21]. S. Das Sarma, S. Adam, E. H. Hwang, and E. Rossi, Rev. Mod. Phys. **83**, 407 (2011).

[22]. [E. McCann and V.I. Falko, Physical Review Letters 96, 086805(2006)]

[23]. [Mattias Braun, Luca Chirolli and Guido Burkard, Physical Review **B** **77**, 115433 (2008)]

[24]. [T. Chakraborty and P. Pietiläinen, The Quantum Hall Effects, 2nd edition (Springer, New York, 1995)]

[25]. [R.B. Laughlin, Rev. Mod. Phys **71**, 863 (1999)]

[26]. [J.M. Pereira Jr., F.M. Peeters, P. Vasilopoulos, Phys. Rev. B **76**, 115419(2007)]

[27]. [D.S.L. Abergel, T. Chakraborty, Phys. Rev. Lett. 102, 056807(2009)]

[28]. [M. Mucha - Kruczynski, I.L. Aleiner, V.I. Falko, Phys. Rev. B **84**, 041404(R) (2011)].

[29]. [V.M. Apalkov and T. Chakraborty, Phys. Rev. Lett. **105**, 036801 (2010)]

[30]. [Dean C. R., Young A. F., Meric I., Lee C., Wang L., Sorgenfrei S., Watanabe K., Taniguchi T., Kim P., Shepard K. L. and Hone J., Nature Nanotech **5**, 722(2010)]

[31]. [Ghosh S., Bao W., Nika D. L., Subrina S., Pokatilov E. P., Lau C. N. and Balandin A. A., Nature Materials **9**, 555(2010)]

[32]. [Balandin A. A., Nature Materials **10**, 569(2011)]

[33]. [Ohta T., Bostwick A., Seyller T., Horn K. and Rotenberg E., Science **313**, 951(2006)]

[34]. [Neek-Amal M. and Peeters F. M. Phys. Rev. B **81**, 235421(2010)]

[35]. [Zhang Y. Y., Wang C. M., Cheng Y. and Xiang Y., Carbon **49**, 4511(2011)]

[36]. [Nair R. R., Blake P., Grigorenko A. N., Novoselov K. S., Booth T. J., Stauber T., Peres N. M. R. and Geim A. K., Science **320**, 1308(2008)]

[37]. [Bunch J. S., Verbridge S. S., Alden J. S., van der Zande A. M., Parpia J. M., Craighead H. G. and McEuen P. L., Nano Lett. **8**, 2458(2008)]

[38]. [Bae S., Kim H., Lee Y., Xu X., Park J. S., Zheng Y., Balakrishnan J., Lei T., Kim H. R., Song Y. I., Kim Y. J., Kim K. S., Ozyilmaz B., Ahn J. H., Hong B. H. and Iijima S., Nature Nanotech. **5**, 574(2010)]

[39]. [Xia F., Farmer D. B., Lin Y. M. and Avouris P., Nano Lett. **10**, 715(2010)]

[40]. [Wang C. R., Lu W.S., Hao L., Lee W. L., Lee T. K., Lin F., Cheng I. C. and Chen J. Z., Phys. Rev. Lett. **107**, 186602(2011)]

[41]. [Yan H., Li X., Chandra B., Tulevski G., Wu Y., Freitag M., Zhu W., Avouris P. and Xia F., Nature Nanotech. **7**, 330(2012)]

[42]. [Yan J., Kim M. H., Elle J. A., Sushkov A. B., Jenkins G. S., Milchberg H. M., Fuhrer M. S. and Drew H. D., Nature Nanotech. **7**, 472(2012)]

[43]. [Sugawara K., Kanetani K., Sato T. and Takahashi T., AIP Adv. **1**, 022103(2011)]

[44]. [Kanetani K., Sugawara K., Sato T., Shimizu R., Iwaya K., Hitosugi T. and Takahashia T., Proc. Nat. Acad. Sci. **109**, 19610(2012)]

[45]. [Gong L., Young R. J., Kinloch I. A., Riaz I., Jalil R. and Novoselov K. S., ACS Nano **6**, 2086(2012)]

[46]. [Young R. J., Kinloch I. A., Gong L. and Novoselov K. S., Compos. Sci. Technol. **72**, 1459(2012)]

[47]. [A. Tzalenchuk, S. Lara-Avila, A. Kalaboukhov, S. Paolillo, M. Syvajarvi, R. Yakimova, O. Kazakova, T. Janssen, V. Fal'ko, and S. Kubatkin, Nature Nanotechnology **5**, 186 (2010)]

Declaration

I hereby declare that this thesis is my original work and has not been presented for a degree in any other university. All sources of material used for the thesis have been duly acknowledged.

Name: Belayneh Sewnet

Signature: ....

This thesis has been submitted for the examination with my approval as university advisor.

Name: Prof. Vadim N.Mal'nev

Signature: ....

Addis Ababa University

Department of Physics

June, 2014